Journal of
Applied Crystallography
ISSN 0021-8898

Received 16 August 2006
Accepted 7 December 2006

Small-angle X-ray scattering from polystyrene polymacromonomers with relatively short main chains

Yo Nakamura

Department of Polymer Chemistry, Kyoto University, Katsura, Kyoto 615-8510, Japan. Correspondence e-mail: yonaka@molsci.polym.kyoto-u.ac.jp

Synchrotron small-angle X-ray scattering measurements were made on polystyrene polymacromonomers F33 and F110 with 33 and 110 styrene residues, respectively, in each side chain in toluene at 298.2 K and cyclohexane at 307.7 K. Two F33 samples with different weight-average degrees of polymerization of main chain N_w of 37 and 17 (F33-13 and F33-14, respectively) and two F110 samples with N_w of 61 and 27 (F110-10 and F110-11, respectively) were used. The z-average mean-square radii of gyration of these polymacromonomers were explained by the wormlike chain with finite diameter when we considered the contribution of side chains near the main chain to the contour length. This model was also applied to calculate the particle scattering function $P(\theta)$, giving satisfactory agreements between calculated and experimental $k^2P(\theta)$ for F33-13 and F110-10 plotted against the magnitude of the scattering vector $k = (4\pi/\lambda_0)\sin(\theta/2)$, where λ_0 and θ denote the wavelength of the incident X-ray and the scattering angle, respectively. The data for F33-14 and F110-11, which have short main chains relative to the side chains, cannot be explained by the same model. However, these data were closely fitted by the theoretical values for a comb polymer model with semiflexible main and side chains. The stiffness parameter for side chains in toluene was larger than that in cyclohexane, suggesting that the side chains in the former solvent are more stretched than those in cyclohexane.

1. Introduction

Polymacromonomer molecules have a comb structure with very high side-chain density. Studies on solution properties of polymacromonomers have shown that these molecules behave as semiflexible chains (Wintermantel *et al.*, 1994, 1996; Nemoto *et al.*, 1995). We made static and dynamic light scattering and intrinsic viscosity measurements for polystyrene polymacromonomer with the chemical structure shown in Fig. 1 to determine the dependences of the main-chain stiffness parameter λ^{-1} and the chain diameter d on the degree of polymerization of side chain n_s (Terao *et al.*, 1999*a*, 1999*b*, 1999*c*, 2000; Hokajo *et al.*, 2001, 2005; Sugiyama *et al.*, 2007). We also made small-angle X-ray scattering (SAXS) measurements on polystyrene polymacromonomer F15 with $n_s = 15$ to determine the z-average mean-square radius of gyration $\langle S^2\rangle_z$ and the particle scattering function $P(\theta)$ (Amitani *et al.*, 2005; Nakamura *et al.*, 2007), where θ denotes the scattering angle. Through these SAXS studies, it was found that polymacromonomer molecules can be described by the wormlike chain with the Gaussian segment profile within the cross-sectional plain when the degree of polymerization of main chain N is much larger than n_s. However, when N is small, $P(\theta)$ cannot be explained by the same model. To see whether this is owing to the possible effects from short side chains, it was pertinent to do similar measurements on polystyrene polymacromonomers with larger n_s. Here, we made SAXS measurements on polystyrene polymacromonomers with $n_s = 33$ and 113 (F33 and F110, respectively) and N comparable to or less than n_s in toluene at 298.2 K and cyclohexane at 307.7 K. The former solvent is a good solvent while the latter is a theta solvent for polystyrene polymacromonomers (Terao *et al.*, 1999*a*; Hokajo *et al.*, 2001; Sugiyama *et al.*, 2007).

Table 1
Molecular parameters and mean-square radii of gyration for polystyrene polymacromonomers in cyclohexane (CH) at 307.7 K and in toluene (Tol) at 298.2 K.

Sample	$M_w/10^5$	N_w	N_w/n_s	$\langle S^2\rangle_z$ (CH) (nm^2)	$\langle S^2\rangle_z$ (Tol) (nm^2)
F33-13	1.28	37	1.1	16 ± 2	22 ± 2
F33-14	0.543	17	0.5	10.5 ± 0.5	14 ± 0.5
F110-10	6.80	61	0.6	67 ± 6	77 ± 7
F110-11	2.99	27	0.2	60 ± 5	72 ± 7

2. Experimental

2.1. Polymacromonomer samples

Polymacromonomer samples F33-13, F33-14, F110-10, and F110-11 were chosen from previous studies (Terao *et al.*, 1999*a*; Sugiyama *et al.*, 2007). Molecular weights of the macromonomers for F33 and F110 are 3560 and 11900, respectively. Weight average molecular

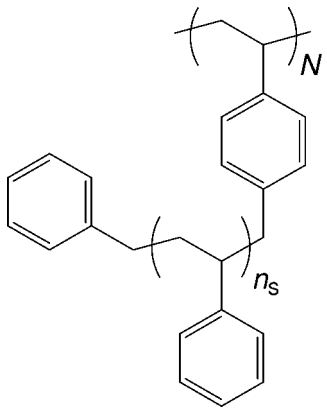

Figure 1
Chemical structure of polystyrene polymacromonomer.

weights M_w, weight-average degrees of polymerization of main chain N_w, and N_w/n_s for the samples studied are summarized in Table 1.

2.2. SAXS measurements

SAXS measurements on toluene (298.2 K) and cyclohexane (307.7 K) solutions were carried out at beamline BL40B2 of the synchrotron facility SPring 8 (Proposal No 2005B0088). The camera length and the wavelength of the incident X-ray λ_0 were set to 1 m and 1.5 nm, respectively. The scattered X-ray was detected on an imaging plate as a two-dimensional image.

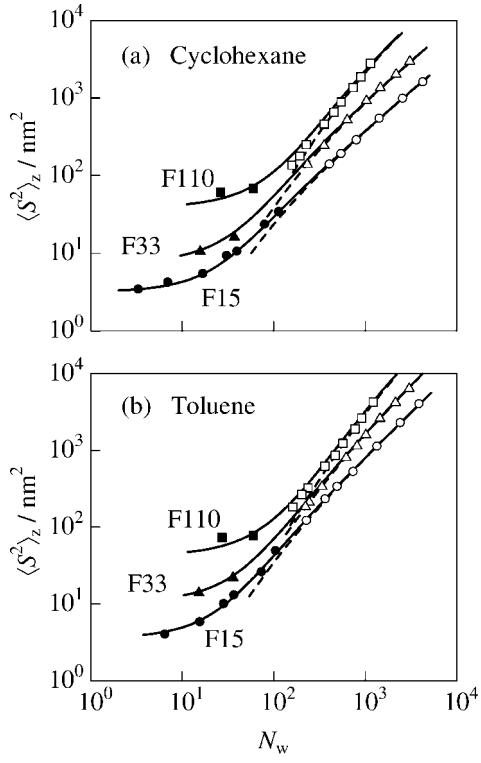

Figure 2
Mean-square radius of gyration determined from SAXS (filled symbols) and light scattering (unfilled symbols) measurements plotted against the degree of polymerization of main chain for the indicated polystyrene polymacromonomers in cyclohexane at 307.7 K (*a*) and in toluene at 298.2 K (SAXS) and 288.2 K (light scattering) (*b*).

A test solution in a quartz glass capillary of 1.5 mm in diameter was kept within ±0.1 K by circulation of temperature-regulated water through a capillary holder. Four solutions with different mass concentrations c were prepared for each sample. Intensity data were accumulated for 5 min for each solution. The solvent intensity was subtracted from the scattering intensity for each solution to obtain the excess intensity $\Delta I(\theta)$ at θ. The resulting $c/\Delta I(\theta)$ at fixed θ was extrapolated to $c = 0$ by means of the square-root plot of $[c/\Delta I(\theta)]^{1/2}$ *vs* c to obtain $[c/\Delta I(\theta)]^{1/2}_{c=0}$. We note that no correction for X-ray absorption by the solution is necessary at infinite dilution. Resulting $[c/\Delta I(\theta)]^{1/2}_{c=0}$ values were plotted against the square of the magnitude of the scattering vector k, which is defined by $(4\pi/\lambda_0)\sin(\theta/2)$. Each plot at small k^2 was fitted by a straight line to obtain the z-average mean-square radius of gyration $\langle S^2\rangle_z$ and the zero scattering angle value $[c/\Delta I(0)]^{1/2}_{c=0}$. The particle scattering function $P(\theta)$ was determined from $[c/\Delta I(0)]_{c=0}/[c/\Delta I(\theta)]_{c=0}$. The $\langle S^2\rangle_z$ values for cyclohexane and toluene solutions are summarized in the fifth and sixth columns, respectively, in Table 1.

3. Results and discussion

3.1. Radius of gyration

The data of $\langle S^2\rangle_z$ from the present SAXS and previous light scattering measurements (Terao *et al.*, 1999*a*, 1999*b*; Sugiyama *et al.*, 2007) are plotted double-logarithmically against N_w in Fig. 2. The figure also includes the previous SAXS results for F15 (Amitani *et al.*, 2005; Nakamura *et al.*, 2007).

The light scattering data for cyclohexane solutions can be fitted by the dashed lines which represent the calculated values of the mean-

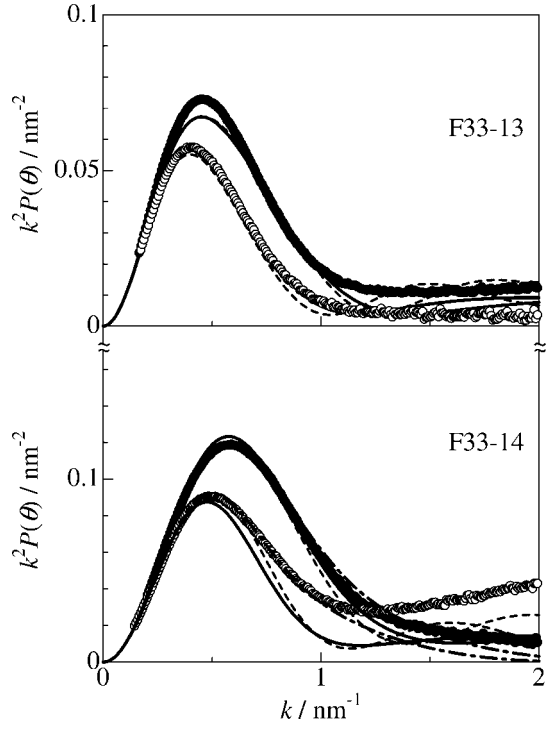

Figure 3
Kratky plots for F33-13 and F33-14 in cyclohexane at 307.7 K (filled circles) and toluene at 298.2 K (unfilled circles).

Table 2
Parameters of polystyrene polymacromonomers in toluene (Tol) at 298.2 K and cyclohexane (CH) at 307.7 K for the calculation of $\langle S^2\rangle$.

Polymacro-monomer	Solvent	λ^{-1} (nm)	M_L (nm^{-1})	B (nm)	d (nm)	δ (nm)
F33	CH	22†	13000†	0	7 ± 0.5	4.0‡
F33	Tol	36†	13800†	18†	8.5 ± 0.5	4.3‡
F110	CH	80§	45500§	0	16 ± 1	9§
F110	Tol	155§	45500§	0	17 ± 1	11§

† Terao *et al.*, 1999*a*; 1999*b*. ‡ Terao *et al.*, 1999*c*; 2000. § Sugiyama *et al.*, 2007.

Table 3
Parameters of polystyrene polymacromonomers in toluene (Tol) at 298.2 K and cyclohexane (CH) at 307.7 K for the calculation of $P(\theta)$.

Sample	Solvent	d (nm)	$\langle r_c^2\rangle^{1/2}$ (nm)	λ_s^{-1} (nm)	d_b (nm)
F33-13	CH	6.5	2.6	–	–
	Tol	7.6	3.0	–	–
F33-14	CH	5.8	2.3	2	3.5
	Tol	7.3	3.0	3	4
F110-10	CH	14	5.7	–	–
	Tol	15	6.4	–	–
F110-11	CH	14	5.7	3	6
	Tol	16	6.4	4	8

square radius of gyration $\langle S^2\rangle$ for the unperturbed wormlike or the Kratky–Porod (KP) chain

$$\langle S^2\rangle_{0,\mathrm{KP}} = \frac{L}{6\lambda} - \frac{1}{4\lambda^2} + \frac{1}{4\lambda^3 L} - \frac{1}{8\lambda^4 L^2}[1 - \exp(-2\lambda L)] \quad (1)$$

where L and λ^{-1} denote the contour length and the stiffness parameter (or the Kuhn segment length), respectively, of the chain. The former parameter can be related to molecular weight M by

$$L = M/M_L \quad (2)$$

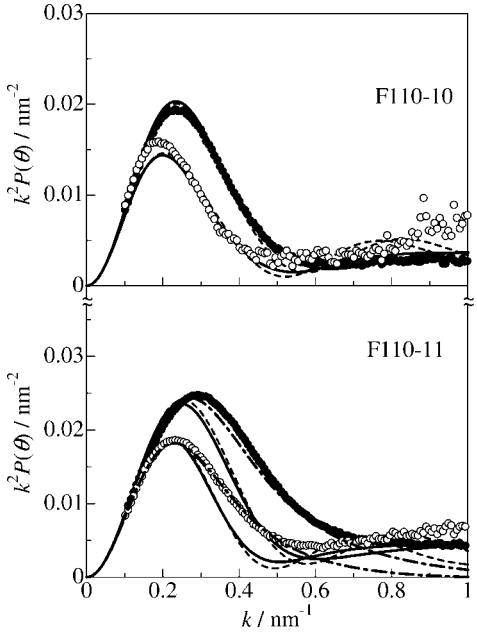

Figure 4
Kratky plots for F110-10 and F110-11 in cyclohexane at 307.7 K (filled circles) and toluene at 298.2 K (unfilled circles).

with the molar mass per unit contour length M_L. The dashed lines for the toluene solutions are calculated from the following equation

$$\langle S^2\rangle_{\mathrm{KP}} = \langle S^2\rangle_{0,\mathrm{KP}}\alpha_S^2 \quad (3)$$

with the radius expansion factor α_S which, according to the quasi two-parameter theory (Yamakawa, 1997), is given by a function of λL and the excluded-volume strength B. We note that the intramolecular excluded-volume effect for F110 in toluene did not need to be considered for its high stiffness of the chain. The parameters for calculation of the dashed lines in Fig. 3 are summarized in Table 2. These lines appreciably deviate downward from the data points at the low molecular weight regions.

Our previous analyses of the data for F15 showed that the effects from the chain thickness and chain ends are essential to explain the data for these regions. The former effect can be taken into account by the following equation.

$$\langle S^2\rangle = \langle S^2\rangle_{\mathrm{KP}} + (d^2/8) \quad (4)$$

The latter effect can be considered by introducing a parameter δ defined by

$$L = M/M_L + \delta \quad (5)$$

Here, δ stands for the apparent contribution of side chains near the main chain ends to L. The δ values were taken from those determined from the intrinsic viscosity (Terao *et al.*, 1999*a*; Sugiyama *et al.*, 2007), while d was chosen so that the calculated values give the closest fit to the experimental values. These values are summarized in the sixth and seventh columns in Table 2.

3.2. Particle scattering function

The particle scattering functions for the samples studied are shown in Figs. 3 and 4 in the manner of the Kratky plot of $k^2P(\theta)$ against k. Each plot has a peak as is expected to thick polymer chains with small axis ratio. The peak top for the cyclohexane solution in each panel is higher than that for the toluene solution. For F33-14, F110-10, and F110-11, $k^2P(\theta)$ of toluene solutions increases at large k while that of cyclohexane solutions is almost independent of k. It is expected that $P(\theta)$ for star polymers in good solvents is proportional to $k^{-5/3}$ at large k (Alessandrini & Carignano, 1992). However, log–log plots of $P(\theta)$ *vs* k for toluene solutions of F33-14 and F110-11 (not shown) gave slopes −1 and −0.5, respectively, at large k, which are much smaller than the predicted value for star polymers in good solvents.

The dashed line for each plot shows the theoretical values for the cylindrical wormlike chain (Nakamura & Norisuye, 2004), where d values summarized in Table 3 were chosen to give the closest fit to the experimental data. These values were determined within ±3% and are about 10% smaller than the d values estimated from $\langle S^2\rangle_z$ in Table 2. The dashed lines in Figs. 3 and 4 fit satisfactorily the experimental data for F33-13 and F110-10 around the peak. However, the tails of dashed lines at large k, $k > 1$ nm^{-1} for F33 and $k > 0.5$ nm^{-1} for F110, swing being different from the straight tails of the data points. To obtain better agreements, we consider the segment density $\rho(r_c)$ in the cross-sectional plain of the polymer by the following Gaussian function.

$$\rho(r_c) = (1/\pi\langle r_c^2\rangle)\exp(-r_c/\langle r_c^2\rangle) \quad (6)$$

Here, r_c and $\langle r_c^2\rangle$ denote the distance from the centre of the plain and the mean-square value of r_c, respectively. The theoretical details for the calculation of $P(\theta)$ are given in Nakamura *et al.* (2007). The solid lines calculated with the $\langle r_c^2\rangle^{1/2}$ values in Table 3 give better fit to the experimental data than the cylindrical wormlike chain. A similar conclusion was given by the small-angle neutron scattering study by

Rathgeber *et al.* (2005) on polymacromonomers with poly(*n*-butylacrylate) side chains. We note that the $\langle r_c^2\rangle^{1/2}$ value for the Gaussian profile for each polymer–solvent system was determined within ±3% and is about 10% larger than the radius for the cylindrical profile which is calculated from $d/8^{1/2}$.

From equation (1), we may calculate $\langle S^2\rangle$ for a linear polystyrene chain with molecular weight twice as large as that of each side chain with λ^{-1} = 2 nm and M_L = 390 nm^{-1} (Norisuye & Fujita, 1982) to obtain $\langle S^2\rangle^{1/2}$ = 2.3 nm and 4.4 nm for F33 and F110, respectively. The former value essentially agrees to the $\langle r_c^2\rangle^{1/2}$ for F33 in cyclohexane, while the latter is smaller than $\langle r_c^2\rangle^{1/2}$ for F110 implying that the side chain of F110 in cyclohexane is rather expanded from its unperturbed dimension. The expansion factor of the side chain in toluene may be calculated from $\langle r_c^2\rangle^{1/2}$ in toluene divided by that in cyclohexane resulting 1.2 and 1.1 for F33 and F110, respectively, which are close to the values known for linear polystyrene in toluene (Abe *et al.*, 1993).

The data points for F33-14 and F110-11 in Figs. 3 and 4 cannot be explained by the models above in which the polymacromonomer molecule is regarded as a thick linear chain. For these polymacromonomers with short main chains comparing to the side chains, this approximate treatment may cease to be valid. Thus, we compare these data with the scattering function $P_0(\theta)$ for comb polymers consisting of infinitely thin semiflexible main and side chains (Amitani *et al.*, 2005). In this model, the side chains with the stiffness parameter λ_s^{-1} are assumed to be connected by free joints to the main chain. However, calculated results gave larger $k^2P_0(\theta)$ than the experimental values especially at large k. Thus, we consider the thickness of the main and side chains according to the following equation for the touched-bead model (Burchard & Kajiwara, 1970).

$$P(\theta) = 9\left(\frac{2}{kd_b}\right)^6[\sin(kd_b/2) - (kd_b/2)\cos(kd_b/2)]^2P_0(\theta) \qquad (7)$$

Here, d_b denotes the bead diameter. The dot–dash lines in Figs. 3 and 4 represent the calculated values for the semiflexible combs with λ_s^{-1} and d_b given in the fifth and sixth columns, respectively, in Table 3. These parameters were chosen to give the closest agreement between the calculated and experimental values, where the main-chain stiffness λ^{-1} was fixed to the values given in Table 2. The dot–dash lines almost perfectly fit the data points except the high-k tails. The λ_s^{-1} values in Table 3 for toluene solutions are larger than those for cyclohexane solutions, showing that the side chains in the good solvent take a more stretched conformation than those in the theta solvent.

The author thanks Dr Ken Terao in Osaka University, and Dr Masashi Osa, Mrs Munehiro Hyakutake, Tomoaki Yoshimura and Hiroyuki Okada in Kyoto University, for their help in SAXS measurements at SPring 8.

References

Abe, F., Einaga, Y., Yoshizaki, T. & Yamakawa, H. (1993). *Macromolecules*, **26**, 1884–1890.

Alessandrini, J. L. & Carignano, M. A. (1992). *Macromolecules*, **25**, 1157–1163.

Amitani, K., Terao, K., Nakamura, Y. & Norisuye, T. (2005). *Polym. J.* **37**, 324–331.

Burchard, W. & Kajiwara, K. (1970). *Proc. R. Soc. London Ser. A*, **316**, 185–199.

Hokajo, T., Hanaoka, Y., Nakamura, Y. & Norisuye, T. (2005). *Polym. J.* **37**, 529–534.

Hokajo, T., Terao, K., Nakamura, Y. & Norisuye, T. (2001). *Polym. J.* **33**, 481–485.

Nakamura, Y., Amitani, K. Sugiyama, M. & Norisuye, T. (2007). *J. Polym. Sci. Part B Polym. Phys.* Submitted.

Nakamura, Y. & Norisuye, T. (2004). *J. Polym. Sci. Part B Polym. Phys.* **42**, 1398–1407.

Nemoto, N., Nagai, M., Koike, A. & Okada, S. (1995). *Macromolecules*, **28**, 3854–3859.

Norisuye, T. & Fujita, H. (1982). *Polym. J.* **14**, 143–147.

Rathgeber, S., Pakula, T., Wilk, A., Matyjaszewski, K. & Beers, K. L. (2005). *J. Chem. Phys.* **122**, 124904.

Sugiyama, M., Nakamura, Y. & Norisuye, T. (2007). *Polym. J.* Submitted.

Terao, K., Hayashi, S., Nakamura, Y. & Norisuye, T. (2000). *Polym. Bull.* **44**, 309–316.

Terao, K., Hokajo, T., Nakamura, Y. & Norisuye, T. (1999*c*). *Macromolecules*, **32**, 3690–3694.

Terao, K., Nakamura, Y. & Norisuye, T. (1999*b*). *Macromolecules*, **32**, 711–716.

Terao, K., Takeo, Y., Tazaki, M., Nakamura, Y. & Norisuye, T. (1999*a*). *Polym. J.* **31**, 193–198.

Wintermantel, M., Gerle, M., Fischer, K., Schmidt, M., Wataoka, I., Urakawa, H., Kajiwara, K. & Tsukahara, Y. (1996). *Macromolecules*, **29**, 978–983.

Wintermantel, M., Schmidt, M., Tsukahara, Y., Kajiwara, K. & Kohjiya, S. (1994). *Macromol. Rapid Commun.* **15**, 279–284.

Yamakawa, H. (1997). *Helical Wormlike Chains in Polymer Solutions*. Berlin: Springer.